Röhl, U., Thomas, D.J., Childress, L.B., and the Expedition 378 Scientists
Proceedings of the International Ocean Discovery Program Volume 378
publications.iodp.org

Expedition 378 summary[1]

U. Röhl, D.J. Thomas, L.B. Childress, E. Anagnostou, B. Ausín, B. Borba Dias, F. Boscolo-Galazzo, S. Brzelinski, A.G. Dunlea, S.C. George, L.L. Haynes, I.L. Hendy, H.L. Jones, S.S. Khanolkar, G.D. Kitch, H. Lee, I. Raffi, A.J. Reis, R.M. Sheward, E. Sibert, E. Tanaka, R. Wilkens, K. Yasukawa, W. Yuan, Q. Zhang, Y. Zhang, A.J. Drury, and C.J. Hollis[2]

[1] Röhl, U., Thomas, D.J., Childress, L.B., Anagnostou, E., Ausín, B., Borba Dias, B., Boscolo-Galazzo, F., Brzelinski, S., Dunlea, A.G., George, S.C., Haynes, L.L., Hendy, I.L., Jones, H.L., Khanolkar, S.S., Kitch, G.D., Lee, H., Raffi, I., Reis, A.J., Sheward, R.M., Sibert, E., Tanaka, E., Wilkens, R., Yasukawa, K., Yuan, W., Zhang, Q., Zhang, Y., Drury, A.J., and Hollis, C.J., 2022. Expedition 378 summary. *In* Röhl, U., Thomas, D.J., Childress, L.B., and the Expedition 378 Scientists, *South Pacific Paleogene Climate*. Proceedings of the International Ocean Discovery Program, 378: College Station, TX (International Ocean Discovery Program). https://doi.org/10.14379/iodp.proc.378.101.2022
[2] **Expedition 378 Scientists' affiliations.**

Contents

Keywords
International Ocean Discovery Program, IODP, *JOIDES Resolution*, Expedition 378, South Pacific Paleogene Climate, Climate and Ocean Change, Site U1553, Campbell Plateau, high–southern latitude, Cenozoic climate history, carbon system dynamics, high CO_2 world, Paleocene, Eocene, Oligocene, chronostratigraphy, perturbations, temperature gradients, ocean circulation, intermediate water formation, hydrologic cycling, biological productivity, ice sheet dynamics, plate motion, wind fields

Core descriptions

Supplementary material

References (RIS)

MS 378-101
Published 6 February 2022

Funded by NSF OCE1326927

1. Abstract

International Ocean Discovery Program (IODP) Expedition 378 was designed to recover the first comprehensive set of Paleogene sedimentary sections from a transect of sites strategically positioned in the South Pacific Ocean to reconstruct key changes in oceanic and atmospheric circulation. These sites would have provided an unparalleled opportunity to add crucial new data and geographic coverage to existing reconstructions of Paleogene climate. Following the ~15 month postponement of Expedition 378 and subsequent port changes that resulted in a reduction of the number of primary sites, testing and evaluation of the research vessel *JOIDES Resolution* derrick in the weeks preceding the expedition determined that it would not support deployment of drill strings in excess of 2 km. Consequently, only one of the originally approved seven primary sites was drilled.

Expedition 378 recovered the first continuously cored, multiple-hole Paleogene sedimentary section from the southern Campbell Plateau at Site U1553. This high–southern latitude site builds on the legacy of Deep Sea Drilling Project Site 277 (a single, partially spot cored hole), providing a unique opportunity to refine and expand existing reconstructions of Cenozoic climate history.

As the world's largest ocean, the Pacific Ocean is intricately linked to major changes in the global climate system. Previous drilling in the low-latitude Pacific Ocean during Ocean Drilling Program Legs 138 and 199 and Integrated Ocean Drilling Program Expeditions 320 and 321 provided new insights into climate and carbon system dynamics, productivity changes across the zone of divergence, time-dependent calcium carbonate dissolution, bio- and magnetostratigraphy, the location of the Intertropical Convergence Zone, and evolutionary patterns for times of climatic change and upheaval. Expedition 378 in the South Pacific Ocean uniquely complements this work with a high-latitude perspective, especially because appropriate high-latitude records are unobtainable in the Northern Hemisphere of the Pacific Ocean.

Expedition 378 provides material from the South Pacific Ocean in an area critical for high-latitude climate reconstructions spanning the early Paleocene to late Oligocene. Site U1553 and the entire corpus of shore-based investigations will significantly contribute to the challenges of the "Climate and Ocean Change: Reading the Past, Informing the Future" theme of the 2013–2023 IODP Science Plan (How does Earth's climate system respond to elevated levels of atmospheric CO_2? How resilient is the ocean to chemical perturbations?). Furthermore, Expedition 378 provides material from the South Pacific Ocean in an area critical for high-latitude climate reconstructions spanning the Paleocene to late Oligocene.

2. Introduction

The South Pacific Paleogene Climate science program originated from International Ocean Discovery Program (IODP) Proposal 567-Full4 (**http://iodp.tamu.edu/scienceops/expeditions/south_pacific_paleogene_climate.html**) with the broad goal to investigate the record of Cenozoic climate and oceanography through a drilling transect in the high-latitude southern Pacific Ocean. The principal drilling targets include sediments deposited during the very warm late Paleocene and early Eocene, including the Paleocene/Eocene boundary and Eocene–Oligocene transition (EOT). These records can help scientists investigate how the Eocene Earth maintained high global temperatures and high heat transport to the polar regions despite receiving near-modern levels of solar energy input. Investigation of the recovered sediments will provide critical constraints on the subpolar Pacific Ocean climate, oceanographic structure, and biogeochemical cycling through much of the Cenozoic. New drilling on the southern Campbell Plateau will enable reconstruction of intermediate water compositions in addition to augmenting the Pacific latitudinal gradient.

3. Background

3.1. Reconstruction of environmental conditions and physical processes in the Paleogene oceans

Seafloor sediments record the broad outlines of the major features of ocean circulation such as water mass distributions; regions of steep gradients in temperature, salinity, and biologic productivity; and the distribution of deepwater masses. Surface water provinces are identified by their salinity and temperature in the modern ocean. Distinct assemblages of planktonic organisms are associated with these provinces; thus, microfossil assemblages of these organisms can be used to define the geographic extent of water masses in premodern sediments (Fontorbe et al., 2017). Divergence of near-surface water usually supports higher organic productivity, which leaves a diagnostic geochemical and micropaleontological fingerprint in the underlying sediments. Steep gradients in the surface ocean are preserved in the records of planktonic microfossil assemblages and mark regions of vigorous near-surface transport as wind-driven open-ocean and boundary currents. Winds that drive these currents may be reconstructed through the geochemical composition of the dust from upwind continental areas after accounting for any volcanic ash contributions (e.g., Rea, 1994; Dunlea et al., 2015).

Present poleward heat transport is divided approximately equally between the atmosphere and the oceans. Wind-driven currents achieve about half of the ocean heat transport, whereas the balance of oceanic heat transport is driven by the overturning circulation. Obviously, all aspects of heat transport must be defined as well as possible in our effort to better understand ocean circulation and the role it plays in times of extremely warm climates. By focusing our efforts on a specific time interval in both the previously drilled equatorial and presently proposed subpolar–polar transects, we can advance reconstructions of meridional Eocene heat transfer along with the circulatory response of the ocean and atmosphere.

3.2. Sea-surface temperatures

One of the primary needs for both atmospheric and oceanic circulation models is robust sea-surface temperature (SST) control. SST data form a major boundary condition for constraining these models, and SST is the most easily observable signal of circulation patterns. Temperature gradients can be measured in a relative sense even if the absolute calibrations are off with respect to the subantarctic or equatorial region.

The early Paleogene (66 to ~34 Ma) was the most recent geologic interval during which atmospheric pCO_2 levels were likely above ~1000 ppm (e.g., Pearson et al., 2009; Pagani et al., 2011; Hönisch et al., 2012; Anagnostou et al., 2016, 2020). Proxy records and models indicate that elevated atmospheric greenhouse gas inventories would have produced higher SSTs (e.g., Inglis et al., 2020).

Multiproxy reconstructions of SSTs confirm these results (Hollis et al., 2019) and imply that tropical SSTs ranged from ~34° to 38°C at ~50 Ma (Pearson et al., 2007; Huber, 2008), SSTs in the high-latitude South Pacific (~55°S) ranged from 20° to 35°C (Bijl et al., 2009; Hollis et al., 2012; Pross et al., 2012; Cramwinckel et al., 2018), and Antarctic/high-latitude SST estimates from Seymour Island off the coast of the Antarctic Peninsula were ~15°C (Ivany et al., 2011).

These SST estimates produce early Paleogene equator-to-pole thermal gradients significantly lower than those of the modern oceans (e.g., Hollis et al., 2009; Lunt et al., 2012). Fully coupled model simulations using strong radiative greenhouse gas forcing yield seasonal thermal gradients that are generally consistent with available proxy data (Huber and Caballero, 2011; Hollis et al., 2012; Lunt et al., 2012; Inglis et al., 2020), whereas simulated meridional temperature gradients are overemphasized and high-latitude precipitation is typically underestimated (Carmichael et al., 2016).

3.3. Ocean circulation

Oceanic meridional overturning circulation (MOC) is a crucial component of the climate system and impacts heat transport, nutrient transport, and global carbon cycling. The operating mode of the MOC was significantly different during the Late Cretaceous and early Paleogene (e.g., Thomas et al., 2014; Hutchinson et al., 2018). In the modern oceans, Antarctica is surrounded by the world's strongest ocean current, the Antarctic Circumpolar Current (ACC), which flows around Antarctica and reaches from the surface to abyssal depths. The current is sufficiently strong to cause erosion and sediment transport near its axis at 50°–55°S (e.g., Goodell et al., 1971; Watkins and Kennett, 1977; Hollister and Nowell, 1991; Barker and Thomas, 2004). The Drake Passage (or Drake Isthmus) separated the abyssal South Atlantic from the abyssal South Pacific during much of the Paleogene (there was likely a shallow connection via the Trans-Antarctic Seaway prior to the opening of the Drake Passage), and it is likely that the South Pacific thermohaline structure was different from that in the South Atlantic. In the early Paleogene, the Southern Ocean was divided into Pacific and Atlantic-Indian sectors because Australia and South America were joined to Antarctica. Both Southern Ocean sectors developed a unique subpolar gyre, and the Pacific sector gyre is known as the proto-Ross Gyre (Huber et al., 2004; Stickley et al., 2004).

An increasing catalog of water mass proxy data combined with state-of-the-art numerical simulations provides a reconstruction of MOC characterized by convection in the South Pacific as well as the North Pacific during the latest Cretaceous through early Paleogene. This reconstruction is supported by fully coupled Global Circulation Model simulations that indicate the "age" of deep water in the Pacific Ocean increased from high to low latitudes in both the South and North Pacific (Hague et al., 2012). Neodymium (Nd) isotope records also suggest that the MOC in the Pacific Ocean was dissimilar and separated from the MOC in the Atlantic Ocean (Thomas et al., 2014).

The evolution of modern Antarctic circulation began with the formation of deepwater passages south of Australia (Tasman Gateway) and through the Scotia Arc (Drake Passage). Data from Ocean Drilling Program (ODP) Leg 189 (Stickley et al., 2004; Bijl et al., 2013) suggest the earliest throughflow of a westbound ACC began at ~49–50 Ma through a southern opening of the Tasmanian Gateway in conjunction with the simultaneous onset of regional surface water and continental cooling (2°–4°C). The timing of subsequent deepening of the Tasman Gateway and Drake Passage still is not well constrained; estimates range from the middle Eocene to early Miocene for the development of circum-Antarctic deepwater passages and the formation of the full ACC (Lawver and Gahagan, 1998, 2003; Barker, 2001; Pfuhl and McCave, 2005; Scher and Martin, 2006). Interestingly, abyssal hiatuses along the thermohaline flow path at the base of the Campbell Plateau developed at the time of the Eocene/Oligocene boundary; however, shallow-water hiatuses indicate a ~3 My younger formation age. Furthermore, grain size, stable isotope, and foraminifer data along the ACC flow path suggest that the ACC developed after the EOT, in the late Oligocene or at the Oligocene/Miocene boundary (Pfuhl and McCave, 2005; Lyle et al., 2007). Uncertainty in the timing of ACC formation compounds the ongoing debate about the potential role of ACC formation on global/regional climate. Site U1553 will contribute to our understanding of the timing of ACC formation as well as the potential impact of ACC formation on climate.

3.4. Water formation and hydrologic cycling

Deep and bottom water likely formed south of the polar front during the Paleogene (e.g., van de Flierdt et al., 2004; Thomas et al., 2014), and the character of this deeper water can be assessed by measuring geochemical signals preserved in benthic foraminifers, fossil fish teeth and bones, and Fe-Mn oxide minerals at the proposed drill sites. Data from Site U1553 will enable us to assess existing models for the evolving mode of intermediate water formation through the Paleogene.

Proxy estimates of atmospheric pCO_2, SSTs, and terrigenous organic matter inputs will contribute significantly to the state of understanding of Paleogene prevailing winds and hydrologic cycling. For example, published model simulations and existing proxy data suggest that overall hydrologic cycling was more intense during the early Paleogene, resulting in higher precipitation in temperate and high latitudes (e.g., Pagani et al., 2006). Higher precipitation/humidity would have caused a greater vegetative cover in temperate and high-latitude continental regions than during drier periods, which in turn would have diminished dust transport from source regions to the ocean basins. Conversely, an enhanced hydrological cycle implies a drying of the arid-to-semiarid regions (Held and Soden, 2006) that may have enhanced the size of the subtropical dust source regions.

Only a few dust accumulation and provenance records exist for the Late Cretaceous and early Paleogene (e.g., Janecek and Rea, 1983; Hovan and Rea, 1992; Zhou and Kyte, 1992; Dunlea et al., 2015). In general, the compilation of long-term data indicates higher dust accumulation in the North Pacific (Deep Sea Drilling Project [DSDP] Site 576; piston Core LL44-GPC3) than the southern Indian Ocean (ODP Sites 756 and 757) during the Late Cretaceous and early Paleogene. Late Paleocene high-resolution data from Indian Ocean DSDP Site 215 indicate a transient increase in dust fluxes at ~59 Ma, but fluxes before and after the pulse seem to be consistent with the few other Southern Hemisphere locations (Hovan and Rea, 1992). Northern Hemisphere dust fluxes increased throughout the Neogene; however, the Indian Ocean sites record a slight decrease in flux throughout the Cenozoic. Site U1553 provides an opportunity to contribute to the record of dust deposition and provenance in the southwestern Pacific, and statistical analysis of bulk sediment elemental data will enable us to determine the accumulation rate of and distinguish between eolian dust and disseminated ash (e.g., Dunlea et al., 2015).

3.5. Chronostratigraphy

High-quality, multiple-hole Cenozoic sedimentary successions from the Atlantic (ODP Legs 171B, 207, and 208 and Integrated Ocean Drilling Program Expedition 342) and Pacific (ODP Legs 198 and 199 and Integrated Ocean Drilling Program Expeditions 320 and 321) yielded high-resolution geochemical records that also led to the development of astronomically calibrated age models (e.g., Röhl et al., 2007; Westerhold et al., 2011, 2018; Littler et al., 2014; Lauretano et al., 2016; Barnet et al., 2019; Westerhold et al., 2020; De Vleeschouwer et al., 2020; Tierney et al., 2020). Expedition 378 will contribute a unique section that includes crucial time intervals for the South Pacific area that will be integrated into the global chronostratigraphy.

3.6. Previous drilling

The best-known Paleogene paleoceanographic site in the South Pacific Ocean is DSDP Site 277, which was drilled during Leg 29. This site is located south of New Zealand and recovered upper Oligocene to upper Paleocene carbonates from a single hole. The Eocene portion of this hole was spot cored with low recovery (Kennett et al., 1975). The current water depth at this location is ~1215 m. The Site 277 sediment sequence consists of ~10 m of Pliocene–Pleistocene carbonate ooze that is disconformably separated from an expanded middle Paleocene to upper Oligocene sequence with sedimentation rates of 19–22 m/My.

The sediments spanning the upper Eocene to upper Oligocene are stiff carbonate oozes, and the ooze–chalk transition is nominally placed at 246 meters below seafloor (mbsf). Middle Paleocene to upper Eocene sediments are variably indurated but typically consist of chalks with low to moderate amounts of lithification (Kennett et al., 1975). Materials from this site provided most of the samples for two classic oxygen isotope curves that first defined the unusually warm early Eocene period (Shackleton and Kennett, 1975; Savin, 1977).

Improvements in advanced piston corer (APC) and half-length APC (HLAPC) technologies have significantly improved the ability to develop triple-core stratigraphic splices. This capacity will allow for unprecedented insight into the details and timing of the major events preserved in the sedimentary record of the Campbell Plateau as reported by Hollis et al. (2015) for DSDP Site 277.

3.7. Seismic studies and site survey data

No modern seismic surveys exist in the immediate vicinity of Site U1553, and the original location definition for Site 277 was based solely on drilling vessel *Glomar Challenger* shipboard subbottom depth profiling (3.5 kHz) (Kennett et al., 1975).

4. Scientific objectives

As laid out in Proposal 567-Full4, Expedition 378 sought to elucidate the temperate to subpolar climate and oceanography of the very warm Eocene, as well as the middle and late Cenozoic, in the far southern Pacific Ocean. Proposed drill sites were positioned along Anomaly 25 (56 Ma) between 56° and 70°S paleolatitudes (using the Ocean Drilling Stratigraphic Network web page backtrack scheme). The overall aim was to obtain a continuous well-preserved sediment section that would address the following primary scientific objectives (of equal priority):

1. To reconstruct the early Eocene surface water temperature gradient around Antarctica to monitor ocean heat transport and to extrapolate subsurface water structure (proposed Sites SP-1B, SP-2B, SP-3B, and DSDP 277 and, to a lesser extent, proposed Sites SP-4B, SP-5B, and SP-15A),
2. To establish the early Eocene vertical temperature gradient (proposed Sites DSDP 277, SP-1B, and SP-2B),
3. To evaluate early Eocene biological productivity and determine nutrient exchange and mixing of surface and subsurface waters (proposed Sites SP-1B, SP-2B, SP-3B, and DSDP 277 and, to a lesser extent, proposed Sites SP-4B, SP-5B, and SP-15A),
4. To track the development and variability of South Pacific thermohaline circulation during the Paleogene (proposed Sites SP-1B, SP-2B, SP-3B, SP-15A, SP-4B, and SP-5B),
5. To document the response of the proto-Ross Gyre (South Pacific subantarctic gyre) to the Paleocene/Eocene Thermal Maximum (PETM) (proposed Sites DSDP 277, SP-1B, SP-2B, and SP-3B and, to a lesser extent, proposed Sites SP-4B, SP-5B, and SP-15A),
6. To reconstruct changes in South Pacific temperature, circulation, and productivity associated with the greenhouse–icehouse transition (Eocene/Oligocene boundary) (proposed Sites SP-1B, SP-2B, SP-3B, SP-13A, SP-14A, and DSDP 277 and, to a lesser extent, proposed Sites SP-4B, SP-5B, and SP-15A),
7. To establish the development of the ACC (proposed Sites SP-14A, SP-13A, DSDP 277, SP-1B, SP-2B, and SP-3B), and
8. To reconstruct the evolution of the Paleogene wind field (proposed Site SP-15A and all other sites).

The obtained sediment sections would also address the following additional objectives:

1. To develop a common chronostratigraphic framework for Paleogene Southern Ocean magnetostratigraphy, biostratigraphy, and cyclostratigraphy (all proposed sites),
2. To resolve geographic distribution of important Paleogene and early Neogene hiatuses in concert with ODP Leg 181 results and DSDP drilling (primarily proposed Sites DSDP 277, SP-1B, SP-2B, SP-3B, SP-13A, and SP-14A),
3. To better determine Paleogene Pacific plate motion (all proposed sites), and
4. To determine, if possible, Paleogene and Neogene development of ice rafting from Antarctica (primarily proposed Site SP-1B).

4.1. Revised scientific objectives for Site U1553

Altered drilling operations for Expedition 378 that eliminated the abyssal sites listed in the *Scientific Prospectus* prompted a significant revision of the scientific objectives. Much of the transit

from Lautoka, Fiji, to Site U1553 was devoted to revisiting laboratory group and individual science plans to ensure that each member of the science party had the ability to contribute to the post-cruise science. All of the science plans were crafted to exploit the new continuously cored, multiple-hole sediment section from Site U1553 to achieve the following revised objectives:

1. To reconstruct the surface and deepwater temperatures and carbon inventory, as well as vertical temperature gradients, through the Paleogene, with particular emphasis on the major events that punctuate this long-term record (e.g., the EOT, Middle Eocene Climatic Optimum [MECO], Eocene Thermal Maximum [ETM] events, Early Eocene Climatic Optimum [EECO], PETM, and Cretaceous/Paleogene [K/Pg] boundary);
2. To develop an integrated chronostratigraphic framework for the Paleogene Southern Ocean including magnetostratigraphy, biostratigraphy, and cyclostratigraphy;
3. To refine our understanding of the Paleogene evolution of seawater chemistry, the role of atmospheric concentrations of CO_2, and ice sheet dynamics;
4. To evaluate Paleogene biological productivity and determine nutrient exchange and mixing of surface and subsurface waters;
5. To track the development and variability of South Pacific Intermediate Water composition and its role in overturning circulation throughout the Paleogene, with emphasis on refining the timing and development of the ACC;
6. To determine, if possible, Paleogene and Neogene development of ice rafting from Antarctica;
7. To better determine Paleogene Pacific plate motion; and
8. To reconstruct the evolution of the Paleogene wind field.

5. Site U1553

5.1. Background and objectives

Site U1553 is located at 1221 m water depth and provided the opportunity to continuously core multiple holes of a critical sequence of Paleogene sediments on the southern Campbell Plateau (Figure F1). The objectives of Site U1553 were the overall expedition objectives reported above: to recover a multiple-cored, continuous Paleogene sequence to reconstruct SSTs and deepwater temperatures, as well as vertical temperature gradients, with particular emphasis on the major events that punctuate the Paleogene record (e.g., EOT, MECO, EECO, ETM events, PETM, and K/Pg boundary); to

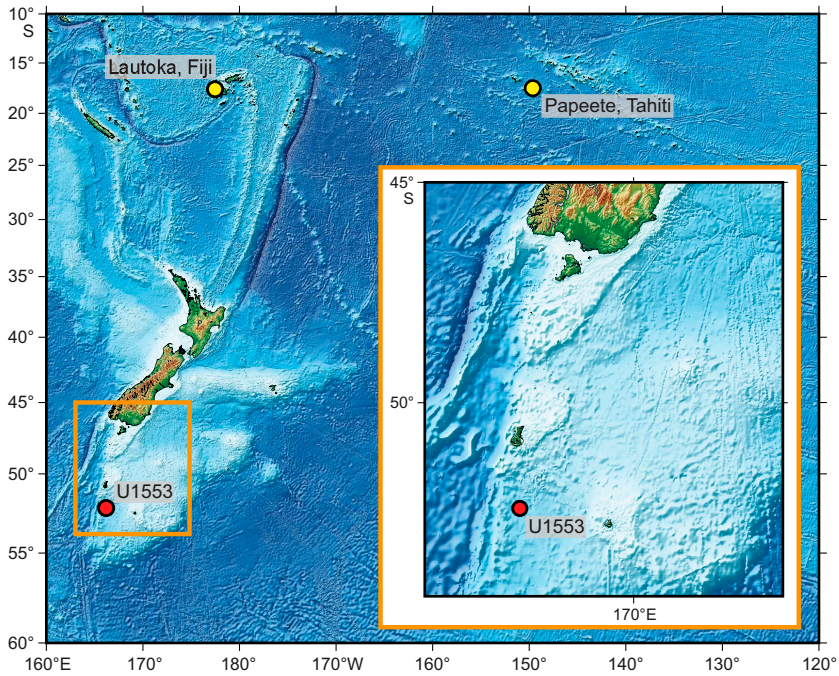

Figure F1. Location of Expedition 378 ports and Site U1553.

develop a common chronostratigraphic framework for Paleogene Southern Ocean magnetostratigraphy, biostratigraphy, and cyclostratigraphy; to refine our understanding of the evolution of seawater chemistry; to evaluate Paleogene biological productivity and determine nutrient exchange and mixing of surface and subsurface waters; and to track the development and variability of South Pacific Intermediate Water composition and its role in overturning circulation during the Paleogene and Late Cretaceous, with emphasis on refining the timing and development of the ACC.

5.2. Operations

After a 2249 nmi transit from Lautoka, Fiji, the vessel stabilized over Site U1553 at 1210 h (all times are local; UTC + 13 h) on 15 January 2020. Five holes were cored at Site U1553 (Figure **F1**; Table **T1**). The operations plan was to triple core the upper portion of the sedimentary sequence using the APC/extended core barrel (XCB) drill string and then rotary core two deep holes to a maximum depth of 670 mbsf, followed by logging of the final hole. Hole U1553A recovered 27 cores taken over a 216.4 m interval with 98.9% recovery. Temperature measurements were taken using the advanced piston corer temperature (APCT-3) tool on Cores 378-U1553A-4H, 7H, and 10H, and all full-length APC cores were oriented using the Icefield MI-5 core orientation tool. The total time spent on Hole U1553A was 34.00 h (1.4 days). After repairs to the top drive brake were concluded, operations resumed at 0915 h on 17 January. Hole U1553B recovered 29 cores taken over a 243.0 m interval with 95.4% recovery. The total time spent on Hole U1553B was 42.50 h (1.8 days), with 10 h spent repairing the top drive. With weather systems moving in, the third APC/XCB hole was deferred in favor of an attempt to reach the deeper objectives with the rotary core barrel (RCB) system. Hole U1553C was spudded at 0010 h on 19 January and drilled ahead without core recovery to 234.0 mbsf. A total of 43 cores were taken over a 333.5 m interval with 47.4% recovery. Anomalously low C_1/C_2 ratios in Cores 43R and 44R forced termination of coring at 567.5 mbsf. The total time spent on Hole U1553C was 82.75 h (3.4 days). Hole U1553D was drilled ahead to 178.3 mbsf. The center bit was pulled, and the Sediment Temperature 2 (SET2) tool was lowered to obtain a fourth temperature measurement with the goal of refining the thermal gradient at Site U1553. After recovering the SET2 temperature probe, the center bit was deployed again and the hole was drilled to 399.4 mbsf. During coring operations, clearance was provided by the Environmental Protection and Safety Panel to advance Hole U1553D deeper than Hole U1553C on a core-by-core basis pending headspace gas analysis. Hole U1553D was terminated at 584.3 mbsf, and the vessel was offset 20 m west for Hole U1553E. Hole U1553E was spudded at 0845 h on 25 January. A total of 27 cores were taken in Hole U1553E over a 237.6 m interval with 88.3% recovery. The total depth for Hole U1553E was 237.6 mbsf, and the total time spent on Hole U1553E was 33.25 h (1.4 days). The total time spent at Site U1553 was 11.02 days, which includes 10 h lost to repair of the top drive. The vessel then began the 531 nmi transit to Timaru, New Zealand, to pick up fuel filters before continuing to Papeete, Tahiti (French Polynesia). The detour to Timaru added ~13 h to the originally planned transit to Papeete.

5.3. Principal results

Coring at Site U1553 reached a maximum depth of 584.3 mbsf and recovered a 581.16 m long sedimentary succession of deep-sea pelagic sediment of Pleistocene and Oligocene to early Paleocene age from the Campbell Plateau. The recovered sections comprise five lithostratigraphic units (Figure **F2**). About 4 m of Pleistocene foraminifer-rich nannofossil ooze (Unit I) overlies an

Table T1. Hole summary, Expedition 378. DSF = drilling depth below seafloor. APC = advanced piston corer, HLAPC = half-length APC, XCB = extended core barrel, RCB = rotary core barrel. **Download table in CSV format.**

Hole	Latitude	Longitude	Water depth (m)	Penetration DSF (m)	Interval cored (m)	Core recovered (m)	Recovery (%)	Drilled interval (m)	Total cores (*N*)	APC cores (*N*)	HLAPC cores (*N*)	XCB cores (*N*)	RCB cores (*N*)	Time on hole (days)
U1553A	52°13.4294′S	166°11.4801′E	1221	216.4	216.4	214.0	99		27	19	2	6	0	1.4
U1553B	52°13.4300′S	166°11.4964′E	1222	243.0	243.0	231.9	95		29	16	0	13	0	1.8
U1553C	52°13.4412′S	166°11.4975′E	1222	567.5	333.5	158.8	48	234.0	43	0	0	0	43	3.5
U1553D	52°13.4403′S	166°11.4796′E	1222	584.3	184.9	98.0	53	399.4	19	0	0	0	19	2.9
U1553E	52°13.4409′S	166°11.4616′E	1221	237.6	237.6	209.8	88		27	15	0	12	0	1.5
		Totals:		1848.8	1215.4	912.4	77	633.4	145	50	2	31	62	11.0

expanded sequence (~200 m thick) of late Oligocene–early Oligocene nannofossil ooze with foraminifers (Unit II). The nannofossil ooze in Unit II gradually transitions into nannofossil chalk in Unit III over 50 m from ~175 to 225 mbsf. Lithification of carbonates continues downcore and results in limestone, categorized as Unit IV. Finally, the bottom ~100 m of the sediment column contains siliciclastic Unit V, characterized by alternating mudstone, sandy mudstone, and very fine to medium-grained sandstone (Figure **F3**).

5.3.1. Biostratigraphy

A thin veneer of Pleistocene sediments overlies a sedimentary succession that spans the early late Oligocene to early Paleocene. The upper portion of this succession (Units I–III) is an expanded ~250 m thick Oligocene to late Eocene (including the EOT) interval characterized by high abun-

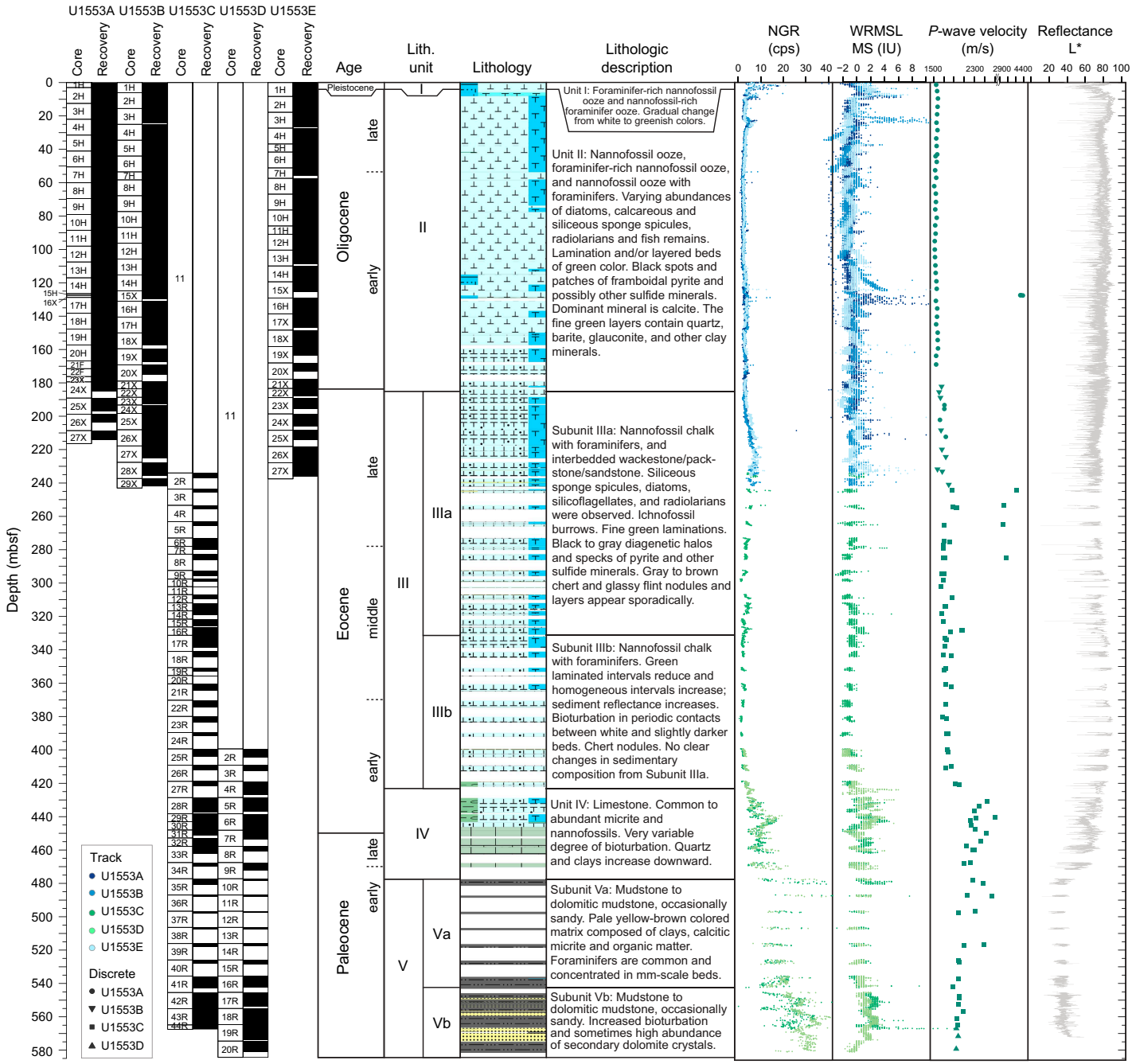

Figure F2. Lithologic summary, Site U1553. NGR = natural gamma radiation, cps = counts per second, WRMSL = Whole Round Multisensor Logger, MS = magnetic susceptibility.

dance and good preservation of all microfossil groups reported here, namely calcareous nannofossils, foraminifers, dinocysts, and radiolarians (Figure **F4**). Diatoms and sponge spicules are also abundant and well preserved throughout this interval. The Eocene and Paleocene intervals in Units IV and V are less expanded and have more variable microfossil abundance and preservation, but biostratigraphic and lithologic evidence indicates the presence of the Paleocene/Eocene boundary. Low calcareous and siliceous microfossil abundance and poor preservation in the basal mudstone to dolomitic mudstone, occasionally sandy unit (V) hampers exact age determination of the basal part of the section (Figure **F4**).

All planktonic microfossil groups lack the low-latitude species that form the basis of standard zonation schemes. For this reason, correlation and age assignments are based primarily on Southern Ocean and Southwest Pacific zonations. The shipboard integrated biozonation for the five holes exhibits overall good agreement between observed bioevents in different microfossil groups.

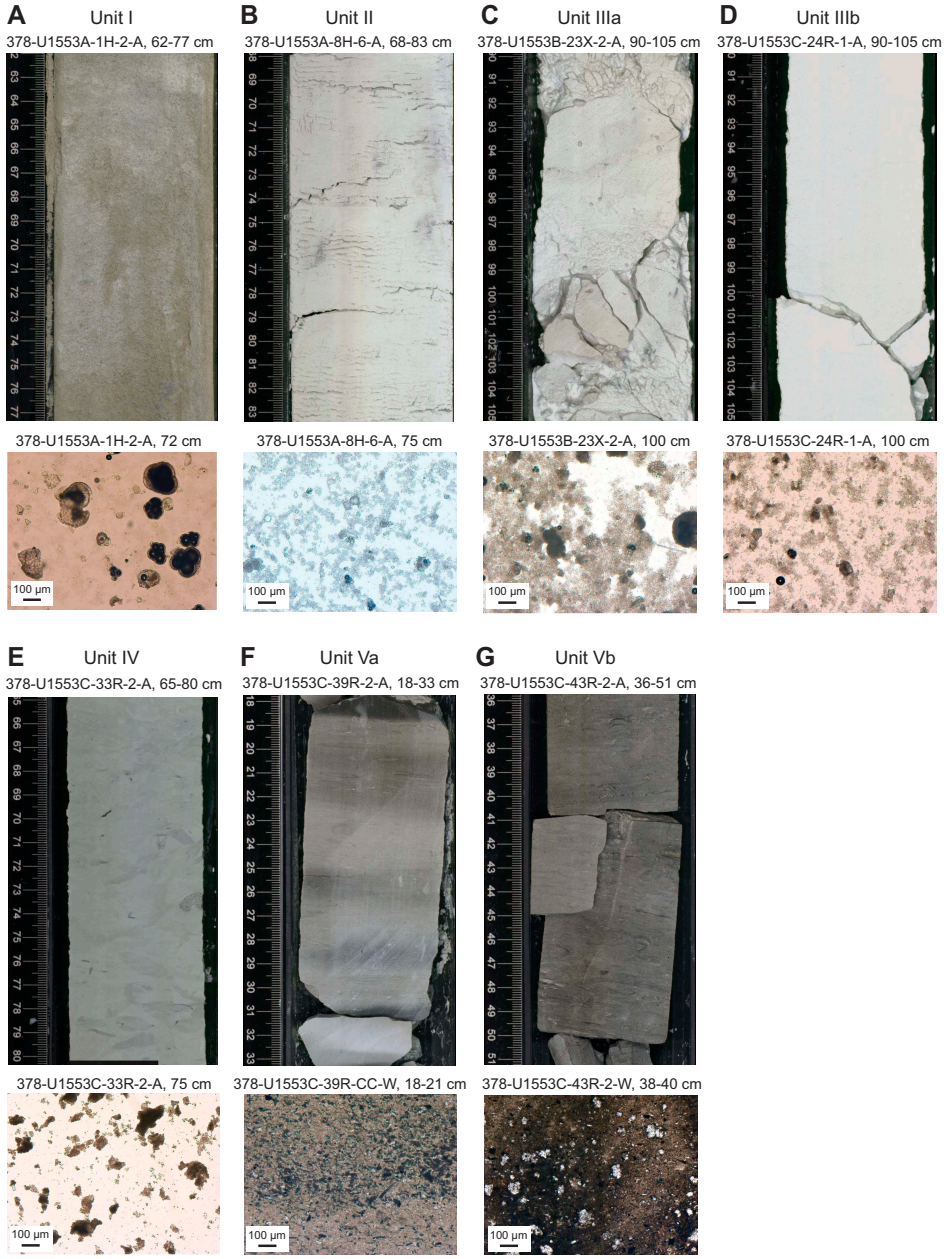

Figure F3. Core photos of representative lithologies of units and subunits with (A–E) typical smear slide photomicrographs and (F, G) plane-polarized thin light sections, Site U1553.

5.3.2. Paleomagnetism

Much of the recovered section was characterized by a very low abundance of magnetic carriers. The high abundance of carbonate in Units I–IV could have diluted the abundance of magnetite, hence contributing to weak overall remanence magnetization. Consequently, only the uppermost 125 m of Hole U1553A was suitable for magnetostratigraphic reconstruction. This preliminary magnetostratigraphy for the upper part of Hole U1553A is composed of five pairs of normal and reversed polarity patterns (n1/r1 to n5/r5 downsection).

5.3.3. Geochemistry

The geochemical composition of the sediment and water samples from Site U1553 reflects the lithostratigraphic composition and downcore diagenetic processes (Figure F5). Downcore changes

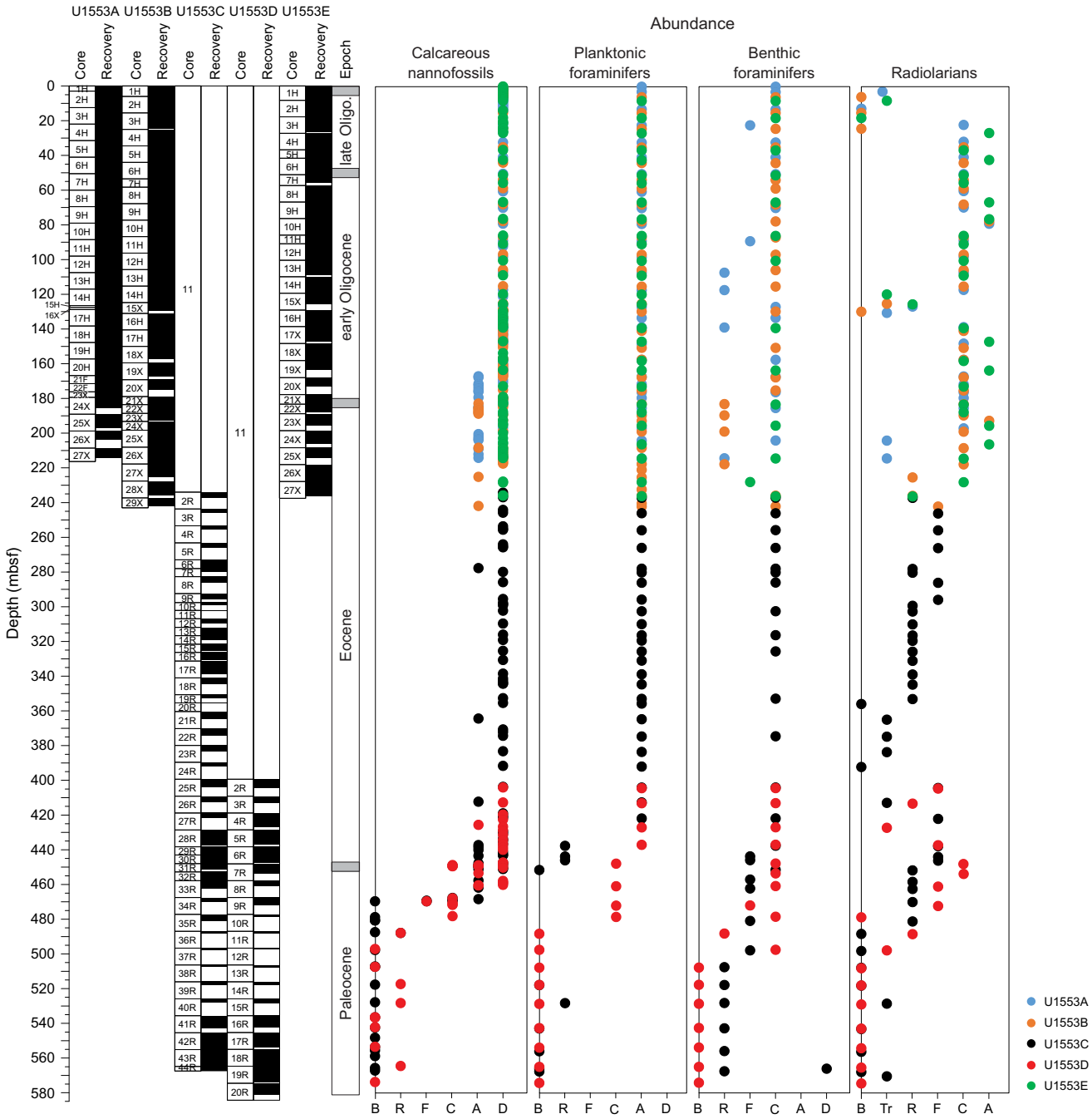

Figure F4. Microfossil abundance, Site U1553. Abundance: D = dominant, A = abundant, C = common, F = few, R = rare, Tr = trace, B = barren.

in the abundance of carbonate and aluminosilicates mirror the lithologic transition between Units IV and V. The presence of occasional glauconite, manganese nodules, pyrite, and chert suggest possible subseafloor changes in the aluminosilicates and the siliceous and carbonaceous components of the sediment. Interstitial water profiles compiled from Site U1553 resolve the first-order diagenetic processes and their potential impact on the application of paleoceanographic proxies.

Headspace gas analyses for the uppermost 480 m of Site U1553 indicate very low hydrocarbon concentrations, suggesting the lack of biogenic and/or thermogenic gas production or their upward migration. A sudden increase in methane concentration occurs at the transition from Unit IV to Unit V. The methane increase is accompanied by the detection of thermogenic hydrocarbons (C_2, C_3, and C_4), suggesting in situ methane production, possibly by microbial activity, and upward migration of thermogenic gas. Gradually decreasing C_1/C_2 ratios with depth led to the termination of drilling operations in Hole U1553C at 568 mbsf. Recalculation of C_1/C_2 ratios and an additional temperature measurement provided a better constraint for the deeper drilling in Hole U1553D.

Interstitial waters sampled from whole-round squeezing of sediment intervals and with Rhizons indicate an increase in total alkalinity from 2.5 mM at the seafloor to 3.6 mM at 200 mbsf. Ammonium increases from ~20 mM at the seafloor to 650–700 mM at 420 mbsf, suggesting organic matter degradation through a series of redox fronts utilizing manganese/iron oxides and sulfate as electron acceptors. Carbonate dissolution/reprecipitation could explain the increase in calcium and strontium with depth. Ba concentrations are <3 µM, possibly suggesting low amounts of sulfate reduction, which, however, increases at depth. K and Mg concentrations decrease downcore, reflecting alteration and uptake into clays formed within the seafloor (e.g., glauconite) or because of uptake into recrystallizing carbonates or authigenic clays forming within the seafloor.

Solid-phase analyses indicate that the sediments predominantly consist of carbonate (average = 90%) for the uppermost 420 m of Site U1553 (Units I–IV), ranging from 78% to 99% (Figure **F5**). Carbonate weight percent drops to <10 wt% at the top of Unit V (~480 mbsf), and this decrease

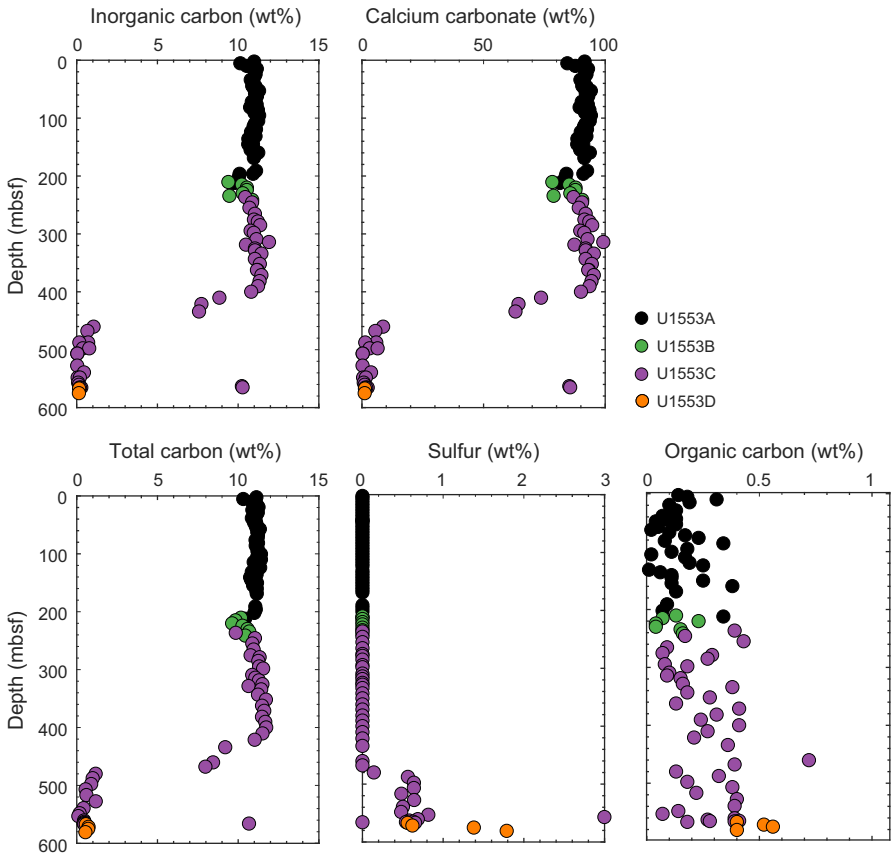

Figure F5. Elemental composition of the solid phase, Site U1553.

coincides with an increase in Al, Si, and trace elements associated with aluminosilicates. Overall, organic carbon content is low (<0.4%). X-ray fluorescence core scanning was undertaken for all cores on shore and provides an unprecedented high-resolution record of elemental intensities for the newly recovered Campbell Plateau Cenozoic sediments.

5.3.4. Physical properties

Variations in physical properties data correspond to transitions between major lithostratigraphic units (Figures F6, F7). A slight increase in bulk density and natural gamma radiation at 180 mbsf corresponds with the transition between Units II and III. A significant increase in *P*-wave velocity and bulk density at 423 mbsf marks the top of Unit IV. A large increase in natural gamma radiation counts, decrease in *P*-wave velocity and bulk density, and change in color at 477 mbsf are reflective of the higher silica and clay content of Unit V.

5.3.5. Stratigraphic correlation

Cores recovered using the APC and XCB coring systems in Holes U1553A, U1553B, and U1553E, although seemingly in good condition and with reasonable recovery rates, were difficult to correlate because of the combined effects of the carbonate-rich lithology, age of the sediments, postdepositional history, and occasional core top drilling disturbance. Preliminary core offsets to align Holes U1553A, U1553B, and U1553E were assigned, but no continuous splice was attempted

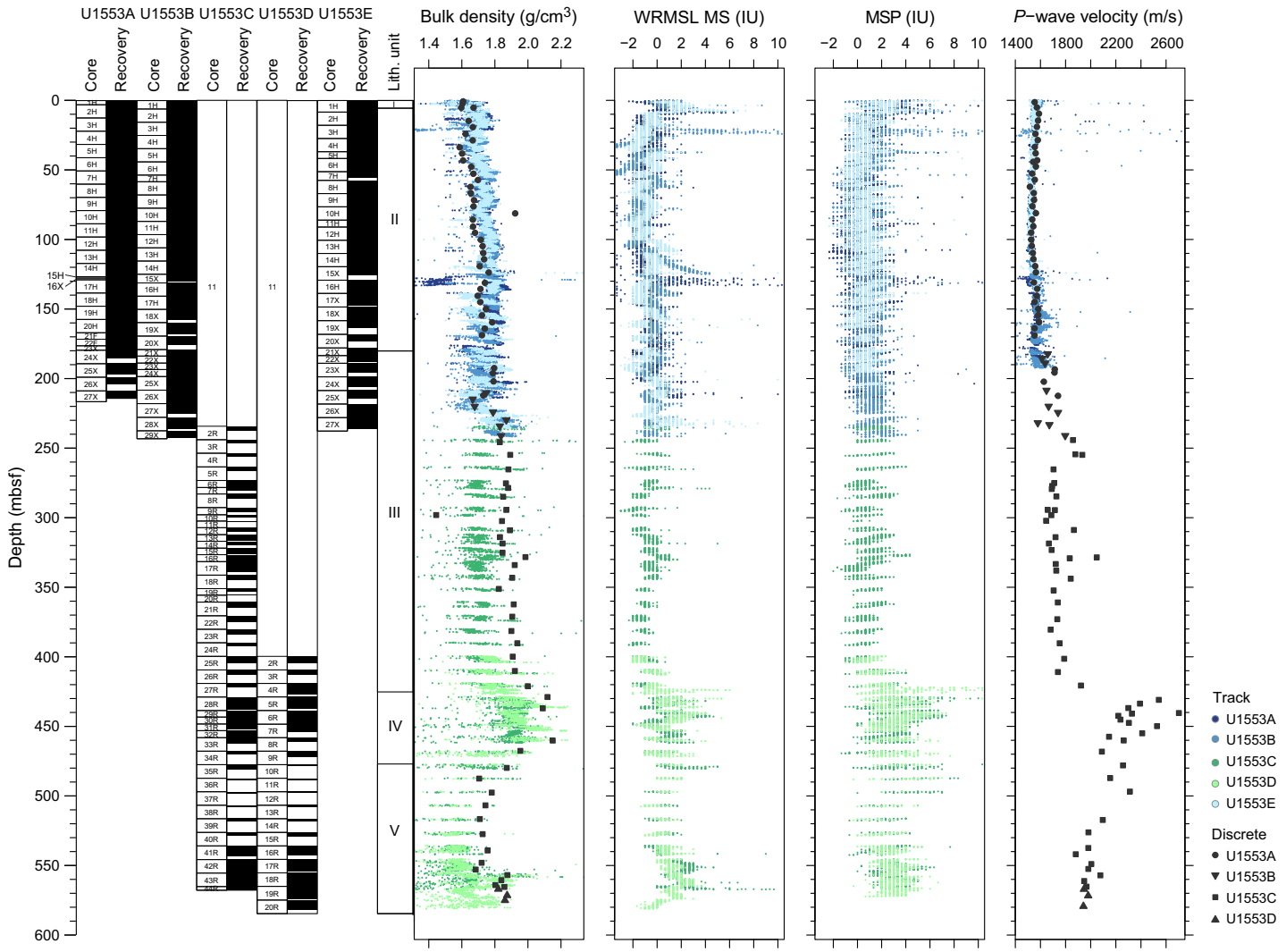

Figure F6. Whole-Round Multisensor Logger (WRMSL)–measured gamma ray attenuation (GRA) and discrete bulk density, WRMSL-measured magnetic susceptibility (MS), Section Half Multisensor Logger (SHMSL)–measured point magnetic susceptibility (MSP), and WRML-measured and discrete *P*-wave velocity, Site U1553. GRA bulk density values for Holes U1553C and U1553D are raw, uncorrected values.

during the expedition. Correlation of the two deeper holes (U1553C and U1553D) drilled using the RCB coring system was not possible for much of the section at the usual meter and decimeter scale because of poor recovery and the recovery of nonoverlapping intervals. An exception was a series of cores surrounding the possible PETM interval and in the early Paleocene. X-ray fluorescence core scanning on shore was crucial for defining a reliable composite section.

6. Preliminary scientific assessment

Expedition 378 recovered five sedimentary sequences from Site U1553 that collectively span an expanded and continuous Oligocene through late Eocene section, a triple-cored EOT, much of the Eocene, a double-cored PETM, and a unique and expanded Paleocene mudstone interval. The K/Pg boundary was a primary target of drilling at Site U1553, and it was not recovered because of the need to terminate Hole U1553D above our maximum approved drilling depth.

Comparison of the recovery from Sites U1553 and 277 indicates substantially more complete records of the Oligocene, much of the Eocene, and much deeper into the Paleocene, even into the earliest Paleogene (Figures **F2**, **F8**). Postcruise analyses employing state-of-the-art proxies will enable us to accomplish most of the revised science objectives presented here and will provide new and refined insights from this first continuously cored, multiple-hole, high–southern latitude Paleogene site.

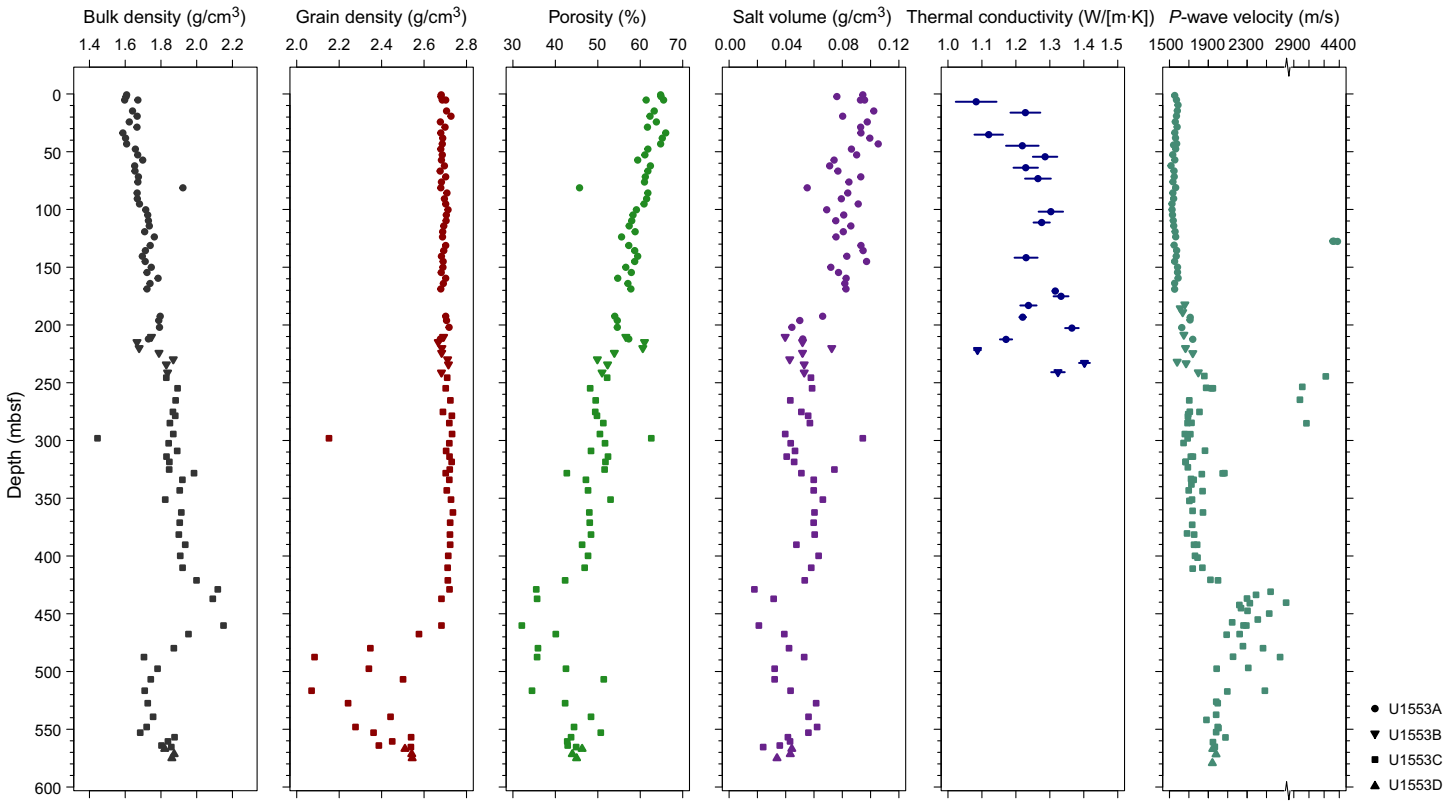

Figure F7. Discrete bulk density, grain density, porosity, salt volume, thermal conductivity, and *P*-wave velocity, Holes U1553A–U1553D. No discrete measurements were taken from Hole U1553E. *P*-wave velocity has a split *x*-axis to show higher *P*-wave velocity measurements in packstone and chert layers.

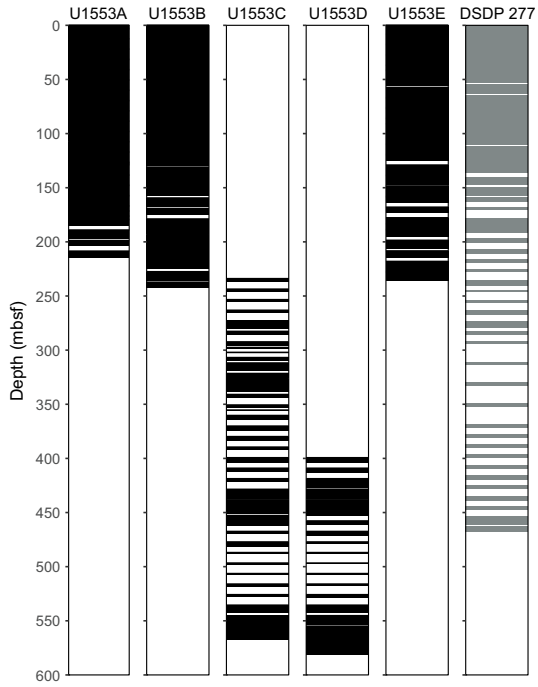

Figure F8. Comparison of Site U1553 and DSDP Site 277 core recovery.

References

Anagnostou, E., John, E.H., Babila, T.L., Sexton, P.F., Ridgwell, A., Lunt, D.J., Pearson, P.N., Chalk, T.B., Pancost, R.D., and Foster, G.L., 2020. Proxy evidence for state-dependence of climate sensitivity in the Eocene greenhouse. *Nature Communications*, 11(1):4436. **https://doi.org/10.1038/s41467-020-17887-x**

Anagnostou, E., John, E.H., Edgar, K.M., Foster, G.L., Ridgwell, A., Inglis, G.N., Pancost, R.D., Lunt, D.J., and Pearson, P.N., 2016. Changing atmospheric CO_2 concentration was the primary driver of early Cenozoic climate. *Nature*, 533(7603):380–384. **https://doi.org/10.1038/nature17423**

Barker, P.F., 2001. Scotia Sea regional tectonic evolution: implications for mantle flow and palaeocirculation. *Earth-Science Reviews*, 55(1):1–39. **https://doi.org/10.1016/S0012-8252(01)00055-1**

Barker, P.F., and Thomas, E., 2004. Origin, signature and palaeoclimatic influence of the Antarctic Circumpolar Current. *Earth-Science Reviews*, 66(1–2):143–162. **https://doi.org/10.1016/j.earscirev.2003.10.003**

Barnet, J.S.K., Littler, K., Westerhold, T., Kroon, D., Leng, M.J., Bailey, I., Röhl, U., and Zachos, J.C., 2019. A high-fidelity benthic stable isotope record of Late Cretaceous-early Eocene climate change and carbon-cycling. *Paleoceanography and Paleoclimatology*, 34(4):672–691. **https://doi.org/10.1029/2019PA003556**

Bijl, P.K., Bendle, J.A.P., Bohaty, S.M., Pross, J., Schouten, S., Tauxe, L., Stickley, C.E., et al., 2013. Eocene cooling linked to early flow across the Tasmanian Gateway. *Proceedings of the National Academy of Sciences of the United States of America*, 110(24):9645–9650. **https://doi.org/10.1073/pnas.1220872110**

Bijl, P.K., Schouten, S., Sluijs, A., Reichart, G.-J., Zachos, J.C., and Brinkhuis, H., 2009. Early Palaeogene temperature evolution of the southwest Pacific Ocean. *Nature*, 461(7265):776–779. **https://doi.org/10.1038/nature08399**

Carmichael, M.J., Lunt, D.J., Huber, M., Heinemann, M., Kiehl, J., LeGrande, A., Loptson, C.A., et al., 2016. A model–model and data–model comparison for the early Eocene hydrological cycle. *Climate of the Past*, 12(2):455–481. **https://doi.org/10.5194/cp-12-455-2016**

Cramwinckel, M.J., Huber, M., Kocken, I.J., Agnini, C., Bijl, P.K., Bohaty, S.M., Frieling, J., et al., 2018. Synchronous tropical and polar temperature evolution in the Eocene. *Nature*, 559(7714):382–386. **https://doi.org/10.1038/s41586-018-0272-2**

De Vleeschouwer, D., Drury, A.J., Vahlenkamp, M., Rochholz, F., Liebrand, D., and Pälike, H., 2020. High-latitude biomes and rock weathering mediate climate–carbon cycle feedbacks on eccentricity timescales. *Nature Communications*, 11(1):5013. **https://doi.org/10.1038/s41467-020-18733-w**

Dunlea, A.G., Murray, R.W., Sauvage, J., Spivack, A.J., Harris, R.N., and D'Hondt, S., 2015. Dust, volcanic ash, and the evolution of the South Pacific Gyre through the Cenozoic. *Paleoceanography and Paleoclimatology*, 30(8):1078–1099. **https://doi.org/10.1002/2015PA002829**

Fontorbe, G., Frings, P.J., De La Rocha, C.L., Hendry, K.R., Carstensen, J., and Conley, D.J., 2017. Enrichment of dissolved silica in the deep equatorial Pacific during the Eocene-Oligocene. *Paleoceanography*, 32(8):848–863. **https://doi.org/10.1002/2017PA003090**

Goodell, H.G., Meylan, M.A., and Grant, B., 1971. Ferromanganese deposits of the South Pacific Ocean, Drake Passage, and Scotia Sea. *In* Reid, J.L. (Ed.), *Antarctic Research Series* (Volume 15): *Antarctic Oceanology I:* Washington, DC (American Geophysical Union), 27–92. **https://doi.org/10.1029/AR015p0027**

Hague, A.M., Thomas, D.J., Huber, M., Korty, R., Woodard, S.C., and Jones, L.B., 2012. Convection of North Pacific Deep Water during the early Cenozoic. *Geology*, 40(6):527–530. **https://doi.org/10.1130/G32886.1**

Held, I.M., and Soden, B.J., 2006. Robust responses of the hydrological cycle to global warming. *Journal of Climate*, 19(21):5686–5699. **https://doi.org/10.1175/JCLI3990.1**

Hollis, C.J., Dunkley Jones, T., Anagnostou, E., Bijl, P.K., Cramwinckel, M.J., Cui, Y., Dickens, G.R., et al., 2019. The DeepMIP contribution to PMIP4: methodologies for selection, compilation and analysis of latest Paleocene and early Eocene climate proxy data, incorporating version 0.1 of the DeepMIP database. *Geoscientific Model Development*, 12(7):3149–3206. **https://doi.org/10.5194/gmd-12-3149-2019**

Hollis, C.J., Handley, L., Crouch, E.M., Morgans, H.E.G., Baker, J.A., Creech, J., Collins, K.S., et al., 2009. Tropical sea temperatures in the high-latitude South Pacific during the Eocene. *Geology*, 37(2):99–102. **https://doi.org/10.1130/G25200A.1**

Hollis, C.J., Hines, B.R., Littler, K., Villasante-Marcos, V., Kulhanek, D.K., Strong, C.P., Zachos, J.C., Eggins, S.M., Northcote, L., and Phillips, A., 2015. The Paleocene–Eocene Thermal Maximum at DSDP Site 277, Campbell Plateau, southern Pacific Ocean. *Climate of the Past*, 11(7):1009–1025. **https://doi.org/10.5194/cp-11-1009-2015**

Hollis, C.J., Taylor, K.W.R., Handley, L., Pancost, R.D., Huber, M., Creech, J.B., Hines, B.R., et al., 2012. Early Paleogene temperature history of the southwest Pacific Ocean: reconciling proxies and models. *Earth and Planetary Science Letters*, 349–350:53–66. **https://doi.org/10.1016/j.epsl.2012.06.024**

Hollister, C.D., and Nowell, A.R.M., 1991. HEBBLE epilogue. *Marine Geology*, 99(3):445–460. **https://doi.org/10.1016/0025-3227(91)90055-9**

Hönisch, B., Ridgwell, A., Schmidt, D.N., Thomas, E., Gibbs, S.J., Sluijs, A., Zeebe, R., et al., 2012. The geological record of ocean acidification. *Science*, 335(6072):1058–1063. **https://doi.org/10.1126/science.1208277**

Hovan, S.A., and Rea, D.K., 1992. Paleocene/Eocene boundary changes in atmospheric and oceanic circulation: a Southern Hemisphere record. *Geology*, 20(1):15–18. **https://doi.org/10.1130/0091-7613(1992)020%3C0015:PEBCIA%3E2.3.CO;2**

Huber, M., 2008. A hotter greenhouse? *Science*, 321(5887):353–354. **https://doi.org/10.1126/science.1161170**

Huber, M., Brinkhuis, H., Stickley, C.E., Doos, K., Sluijs, A., Warnaar, J., Schellenberg, S.A., and Williams, G.L., 2004. Eocene circulation of the Southern Ocean: was Antarctica kept warm by subtropical waters? *Paleoceanography and Paleoclimatology*, 19(4):PA4026. **https://doi.org/10.1029/2004PA001014**

Huber, M., and Caballero, R., 2011. The early Eocene equable climate problem revisited. *Climate of the Past*, 7(2):603–633. **https://doi.org/10.5194/cp-7-603-2011**

Hutchinson, D.K., de Boer, A.M., Coxall, H.K., Caballero, R., Nilsson, J., and Baatsen, M., 2018. Climate sensitivity and meridional overturning circulation in the late Eocene using GFDL CM2.1. *Climate of the Past*, 14(6):789–810. **https://doi.org/10.5194/cp-14-789-2018**

Inglis, G.N., Bragg, F., Burls, N.J., Cramwinckel, M.J., Evans, D., Foster, G.L., Huber, M., et al., 2020. Global mean surface temperature and climate sensitivity of the early Eocene Climatic Optimum (EECO), Paleocene–Eocene Thermal Maximum (PETM), and latest Paleocene. *Climate of the Past*, 16(5):1953–1968. **https://doi.org/10.5194/cp-16-1953-2020**

Ivany, L.C., Brey, T., Huber, M., Buick, D.P., and Schöne, B.R., 2011. El Niño in the Eocene greenhouse recorded by fossil bivalves and wood from Antarctica. *Geophysical Research Letters*, 38(16):L16709. **https://doi.org/10.1029/2011GL048635**

Janecek, T.R., and Rea, D.K., 1983. Eolian deposition in the northeast Pacific Ocean: Cenozoic history of atmospheric circulation. *Geological Society of America Bulletin*, 94(6):730–738. **https://doi.org/10.1130/0016-7606(1983)94<730:EDITNP>2.0.CO;2**

Kennett, J.P., Houtz, R.E., Andrews, P.B., Edwards, A.R., Gostin, V.A., Hajos, M., Hampton, M., Jenkins, D.G., Margolis, S.V., Ovenshine, A.T., and Perch-Nielsen, K., 1975. Cenozoic paleoceanography in the Southwest Pacific Ocean, Antarctic glaciation, and the development of the Circum-Antarctic Current. *In* Kennett, J.P., Houtz, R.E., et al., *Initial Reports of the Deep Sea Drilling Project*, 29: Washington, DC (US Government Printing Office), 1155–1169. **http://hdl.handle.net/10.2973/dsdp.proc.29.144.1975**

Lauretano, V., Hilgen, F.J., Zachos, J.C., and Lourens, L.J., 2016. Astronomically tuned age model for the early Eocene carbon isotope events: a new high-resolution benthic $\delta^{13}C$ benthic record of ODP Site 1263 between ~49 and ~54 Ma. *Newsletters on Stratigraphy*, 49(2):383–400. **https://doi.org/10.1127/nos/2016/0077**

Lawver, L.A., and Gahagan, L.M., 1998. Opening of Drake Passage and its impact on the Cenozoic Ocean. *In* Crowley, T.J., and Burke, K.C. (Eds.), *Tectonic Boundary Conditions for Climate Reconstructions:* Oxford (Oxford University Press), 212–223.

Lawver, L.A., and Gahagan, L.M., 2003. Evolution of Cenozoic seaways in the circum-Antarctic region. *Palaeogeography, Palaeoclimatology, Palaeoecology*, 198(1):11–37. **https://doi.org/10.1016/S0031-0182(03)00392-4**

Littler, K., Röhl, U., Westerhold, T., and Zachos, J.C., 2014. A high-resolution benthic stable-isotope record for the South Atlantic: implications for orbital-scale changes in late Paleocene–early Eocene climate and carbon cycling. *Earth and Planetary Science Letters*, 401:18–30. **https://doi.org/10.1016/j.epsl.2014.05.054**

Lunt, D., Dunkley Jones, T., Heinemann, M., Huber, M., LeGrande, A., Winguth, A., Loptson, C., et al., 2012. A model-data comparison for a multi-model ensemble of early Eocene atmosphere-ocean simulations: EoMIP. *Climate of the Past Discussions*, 8:1229–1273. **https://doi.org/10.5194/cpd-8-1229-2012**

Lyle, M., Gibbs, S., Moore, T.C., and Rea, D.K., 2007. Late Oligocene initiation of the Antarctic Circumpolar Current: evidence from the South Pacific. *Geology*, 35(8):691–694. **https://doi.org/10.1130/G23806A.1**

Pagani, M., Huber, M., Liu, Z., Bohaty, S.M., Henderiks, J., Sijp, W., Krishnan, S., and DeConto, R.M., 2011. The role of carbon dioxide during the onset of Antarctic glaciation. *Science*, 334(6060):1261–1264. **https://doi.org/10.1126/science.1203909**

Pagani, M., Pedentchouk, N., Huber, M., Sluijs, A., Schouten, S., Brinkhuis, H., Sinninghe Damsté, J.S., et al., 2006. Arctic hydrology during global warming at the Palaeocene/Eocene Thermal Maximum. *Nature*, 442(7103):671–675. **https://doi.org/10.1038/nature05043**

Pearson, P.N., Foster, G.L., and Wade, B.S., 2009. Atmospheric carbon dioxide through the Eocene–Oligocene climate transition. *Nature*, 461(7267):1110–1113. **https://doi.org/10.1038/nature08447**

Pearson, P.N., van Dongen, B.E., Nicholas, C.J., Pancost, R.D., Schouten, S., Singano, J.M., and Wade, B.S., 2007. Stable warm tropical climate through the Eocene Epoch. *Geology*, 35(3):211–214. **https://doi.org/10.1130/G23175A.1**

Pfuhl, H.A., and McCave, I.N., 2005. Evidence for late Oligocene establishment of the Antarctic Circumpolar Current. *Earth and Planetary Science Letters*, 235(3–4):715–728. **https://doi.org/10.1016/j.epsl.2005.04.025**

Pross, J., Contreras, L., Bijl, P.K., Greenwood, D.R., Bohaty, S.M., Schouten, S., Bendle, J.A., et al., 2012. Persistent near-tropical warmth on the Antarctic continent during the early Eocene epoch. *Nature*, 488(7409):73–77. **https://doi.org/10.1038/nature11300**

Rea, D.K., 1994. The paleoclimatic record provided by eolian deposition in the deep sea: the geologic history of wind. *Reviews of Geophysics*, 32(2):159–195. **https://doi.org/10.1029/93RG03257**

Röhl, U., Westerhold, T., Bralower, T.J., and Zachos, J.C., 2007. On the duration of the Paleocene–Eocene Thermal Maximum (PETM). *Geochemistry, Geophysics, Geosystems*, 8(12):Q12002. **https://doi.org/10.1029/2007GC001784**

Savin, S.M., 1977. The history of the Earth's surface temperature during the past 100 million years. *Annual Review of Earth and Planetary Sciences*, 5(1):319–355. **https://doi.org/10.1146/annurev.ea.05.050177.001535**

Scher, H.D., and Martin, E.E., 2006. Timing and climatic consequences of the opening of Drake Passage. *Science*, 312(5772):428–430. **https://doi.org/10.1126/science.1120044**

Shackleton, N.J., and Kennett, J.P., 1975. Paleotemperature history of the Cenozoic and the initiation of Antarctic glaciation: oxygen and carbon isotope analyses in DSDP Sites 277, 279, and 281. *In* Kennett, J.P., Houtz, R.E., et al., *Initial Reports of the Deep Sea Drilling Project*, 29: Washington, DC (US Government Printing Office), 743–755. **https://doi.org/10.2973/dsdp.proc.29.117.1975**

Stickley, C.E., Brinkhuis, H., Schellenberg, S.A., Sluijs, A., Röhl, U., Fuller, M., Grauert, M., Huber, M., Warnaar, J., and Williams, G.L., 2004. Timing and nature of the deepening of the Tasmanian Gateway. *Paleoceanography and Paleoclimatology*, 19(4):PA4027. **https://doi.org/10.1029/2004PA001022**

Thomas, D.J., Korty, R., Huber, M., Schubert, J.A., and Haines, B., 2014. Nd isotopic structure of the Pacific Ocean 70–30 Ma and numerical evidence for vigorous ocean circulation and ocean heat transport in a greenhouse world. *Paleoceanography and Paleoclimatology*, 29(5):454–469. **https://doi.org/10.1002/2013PA002535**

Tierney, J.E., Poulsen, C.J., Montañez, I.P., Bhattacharya, T., Feng, R., Ford, H.L., Hönisch, B., et al., 2020. Past climates inform our future. *Science*, 370(6517):eaay3701. **https://doi.org/10.1126/science.aay3701**

van de Flierdt, T., Frank, M., Halliday, A.N., Hein, J.R., Hattendorf, B., Günther, D., and Kubik, P.W., 2004. Deep and bottom water export from the Southern Ocean to the Pacific over the past 38 million years. *Paleoceanography and Paleoclimatology*, 19(1):PA1020. **https://doi.org/10.1029/2003PA000923**

Watkins, N.D., and Kennett, J.P., 1977. Erosion of deep-sea sediments in the Southern Ocean between longitudes 70°E and 190°E and contrasts in manganese nodule development. *In* Heezen, B.C. (Ed.), *Developments in Sedimentology* (Volume 23): *Influence of Abbysal Circulation on Sedimentary Accumulations in Space and Time:* New York (Elsevier), 103–111. **https://doi.org/10.1016/S0070-4571(08)70553-3**

Westerhold, T., Marwan, N., Drury, A.J., Liebrand, D., Agnini, C., Anagnostou, E., Barnet, J.S.K., et al., 2020. An astronomically dated record of Earth's climate and its predictability over the last 66 million years. *Science*, 369(6509):1383–1387. **https://doi.org/10.1126/science.aba6853**

Westerhold, T., Röhl, U., Donner, B., McCarren, H.K., and Zachos, J.C., 2011. A complete high-resolution Paleocene benthic stable isotope record for the central Pacific (ODP Site 1209). *Paleoceanography and Paleoclimatology*, 26(2):PA2216. **https://doi.org/10.1029/2010PA002092**

Westerhold, T., Röhl, U., Donner, B., and Zachos, J.C., 2018. Global extent of early Eocene hyperthermal events: a new Pacific benthic foraminiferal isotope record from Shatsky Rise (ODP Site 1209). *Paleoceanography and Paleoclimatology*, 33(6):626–642. **https://doi.org/10.1029/2017PA003306**

Zhou, L., and Kyte, F.T., 1992. Sedimentation history of the South Pacific pelagic clay province over the last 85 million years inferred from the geochemistry of Deep Sea Drilling Project Hole 596. *Paleoceanography and Paleoclimatology*, 7(4):441–465. **https://doi.org/10.1029/92PA01063**